Fold tightening and strike slip faulting promote meteoric fluid circulation in the Lower Cretaceous carbonates of the Parmelan anticline (Bornes Massif, Western Alps)

Luigi R. Berio[1][*], Silvia Mittempergher[2], Fabrizio Storti[1], Stefano M. Bernasconi[3], Anna Cipriani[2], Federico Lugli[4], Fabrizio Balsamo[1]

(1) Università degli Studi di Parma, Dipartimento di Scienze Chimiche, della Vita e della Sostenibilità Ambientale, NEXT - Natural and Experimental Tectonics Research Group, Parco Area delle Scienze 157/A, 43124 Parma, Italy

(2) Dipartimento di Scienze Chimiche e Geologiche, Università degli Studi di Modena e Reggio Emilia, Via G. Campi 106, 41125 Modena, Italy

(3) Geological Institute, ETH Zürich, Sonneggstrasse 5, Zürich, 8092, Switzerland

(4) Università di Bologna, Dipartimento di Beni Culturali, Via degli Ariani 1, 48121, Ravenna, Italy

*Correspondence: luigiriccardo.berio@studenti.unipr.it

Samples used for in situ MC-ICP-MS analyses and locations of the analysed spots

In the following figures, enlarged images of 11 thick sections are provided with the locations of analysed spots and lines.

Red lines correspond to the locations of Sr isotope analysis. They are labelled with the letter L plus a number which refers to the geochemical dataset provided in Supplementary material, **Table S3**.

Light blue dots correspond to the locations of analysed spots for major and trace elements in syntectonic calcite cements and in Urgonian Limestones and Calcaires gréseux à miches host rocks. The following elements were measured: ^{24}Mg, ^{51}V, ^{55}Mn, ^{57}Fe, ^{85}Rb, ^{88}Sr, ^{89}Y, ^{137}Ba, ^{139}La, ^{140}Ce, ^{141}Pr, ^{146}Nd, ^{147}Sm, ^{153}Eu, ^{157}Gd, ^{159}Tb, ^{163}Dy, ^{165}Ho, ^{166}Er, ^{169}Tm, ^{172}Yb, ^{175}Lu, ^{208}Pb, ^{232}Th, ^{238}U. The numbers refer to the geochemical dataset that is provided in Supplementary material, **Table S6 and Table S7**.

Figure S1 Sample PA3.1. Structural set: V5. Calcite generation: Cal-3.

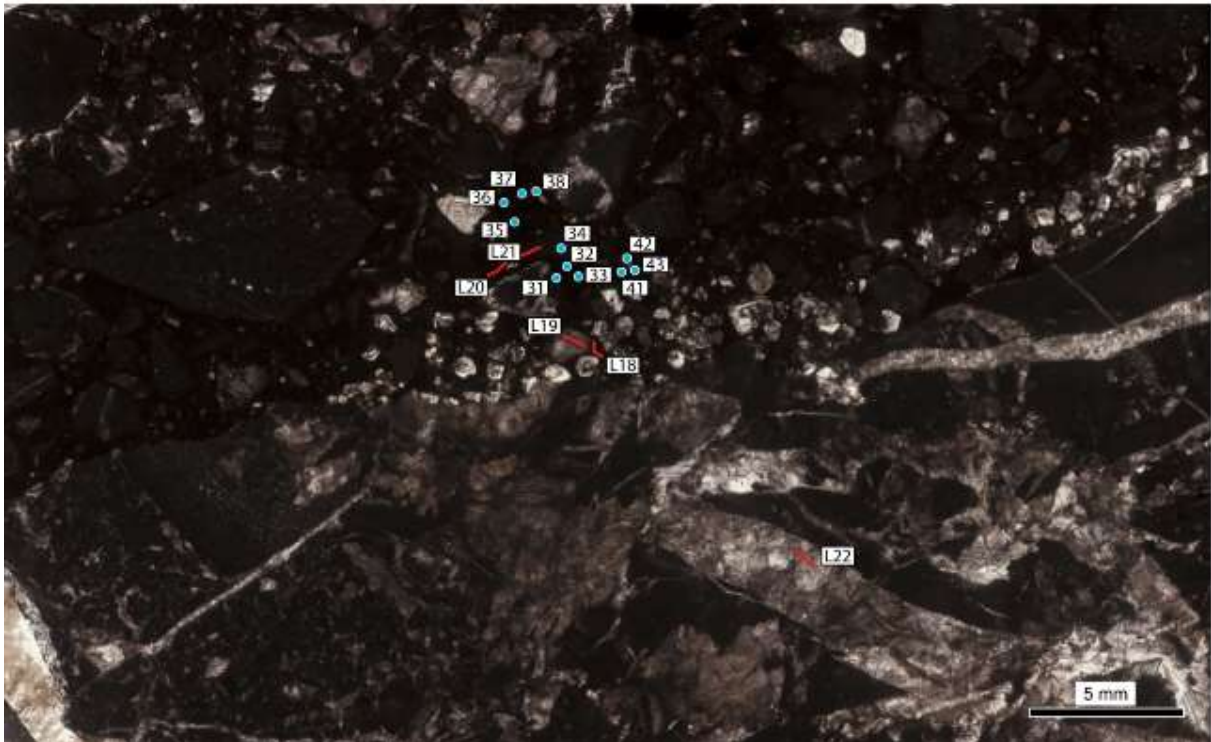**Figure S2** Sample PA3.21. Structural set: CT slickenfibers. Calcite generation: Cal-1 "type".

Figure S3 Sample PA3.25. Fault rock sampled on a transversal fault (TF1). Calcite generation: Cal-4.
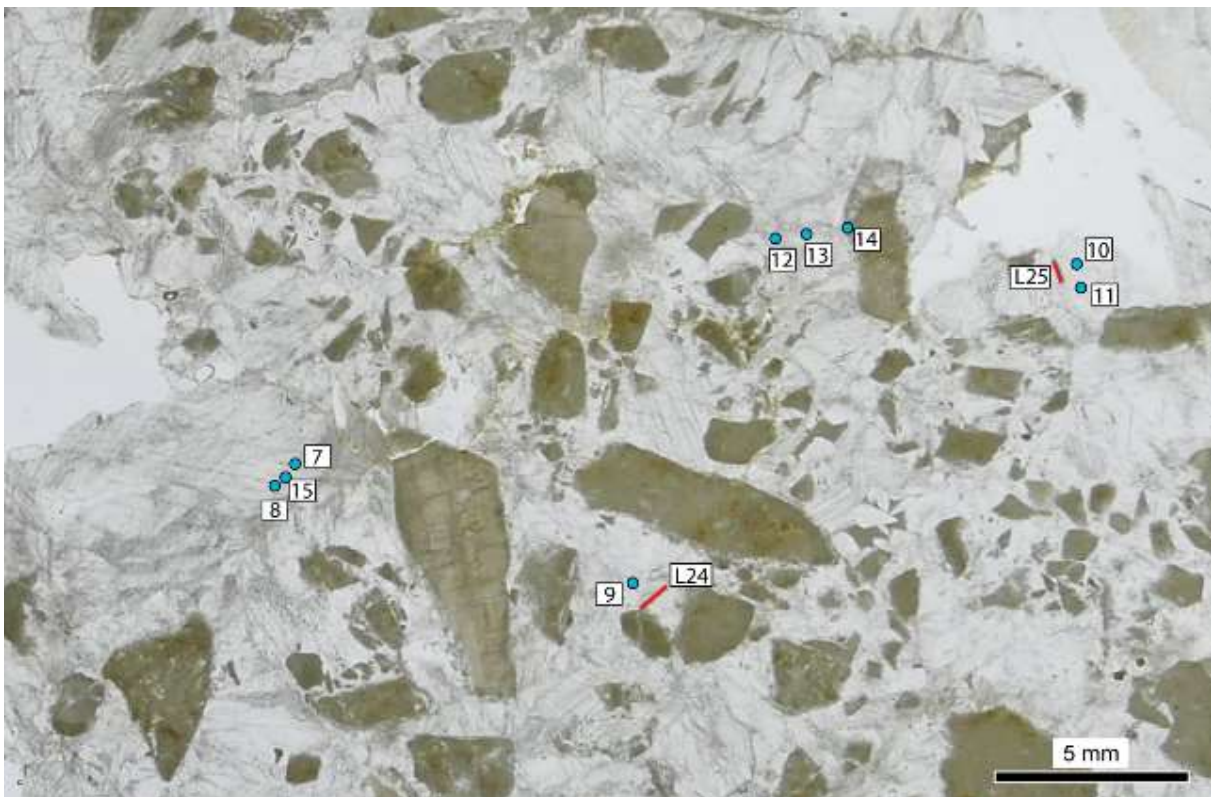

Figure S4 Sample PA5.6. Fault rock sampled on a transversal fault (TF2). Calcite generation: Cal-2.
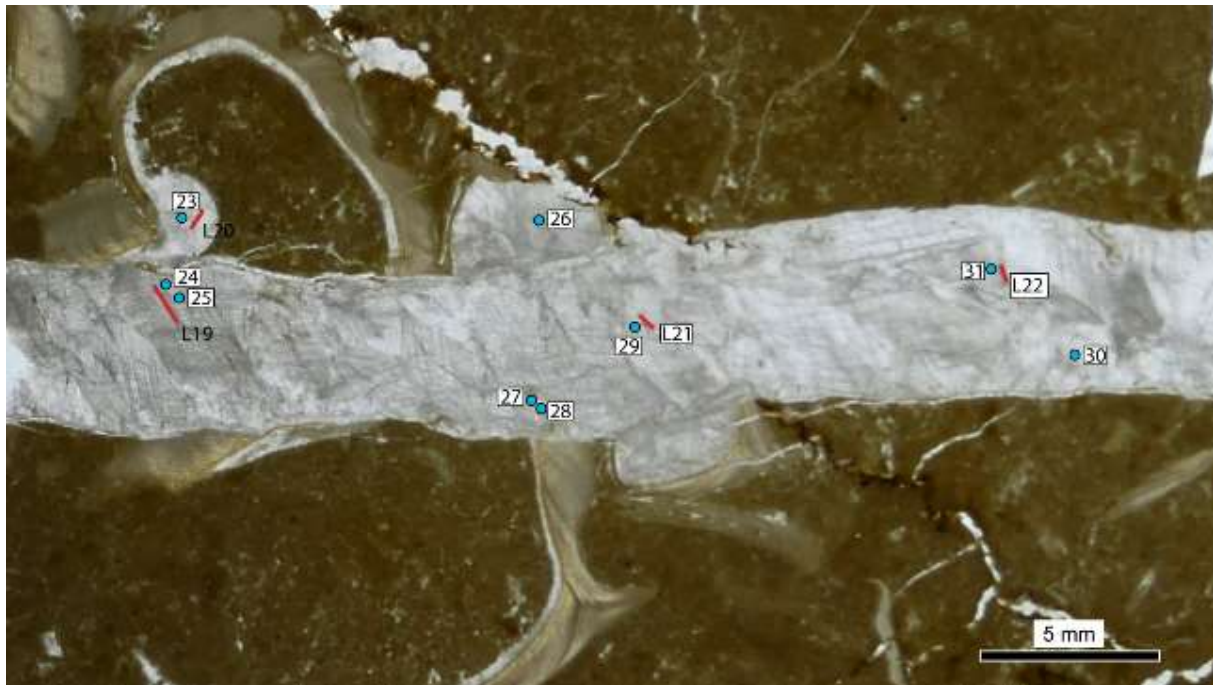
Figure S5 Sample PA5.8. Structural set: V5. Calcite generations: Cal-3 and host rock cement (23 and 26).

Figure S6 Sample PA5.19. Structural set: V1 and V5. Calcite generations: Cal-1a and Cal-2.
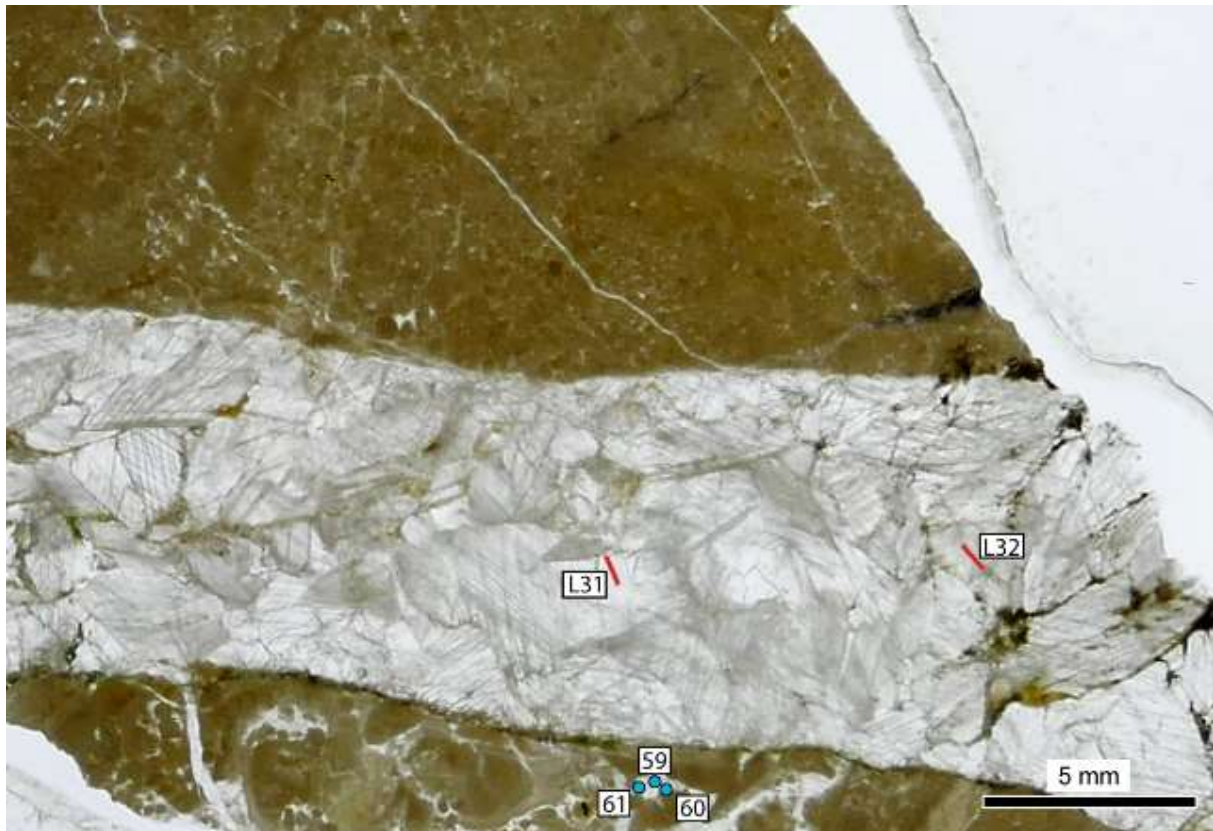
Figure S7 Sample PA6.7. Structural set: V4. Calcite generations: Cal-2 and host rock cements (59, 60, 61).
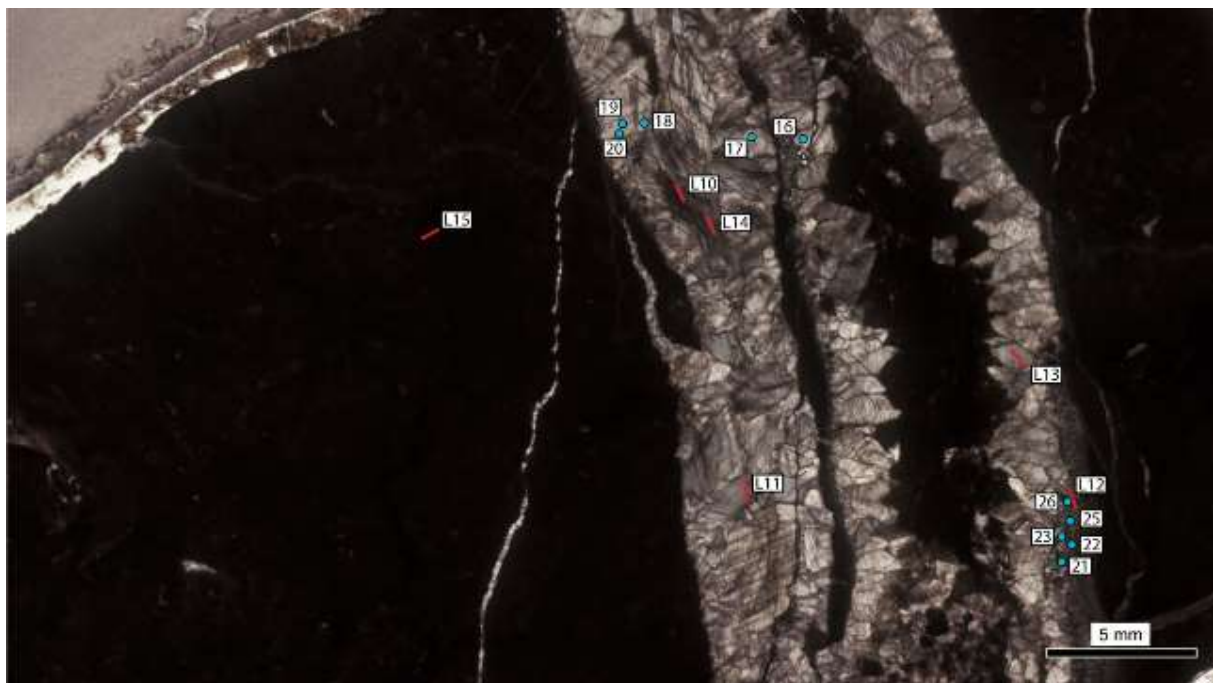

Figure S8 Sample PA6.12. Structural set: V6. Calcite generations: Cal-5.

Figure S9 Sample PA7.27A. Structural set: V1. Calcite generations: Cal-1b and host rock cements.
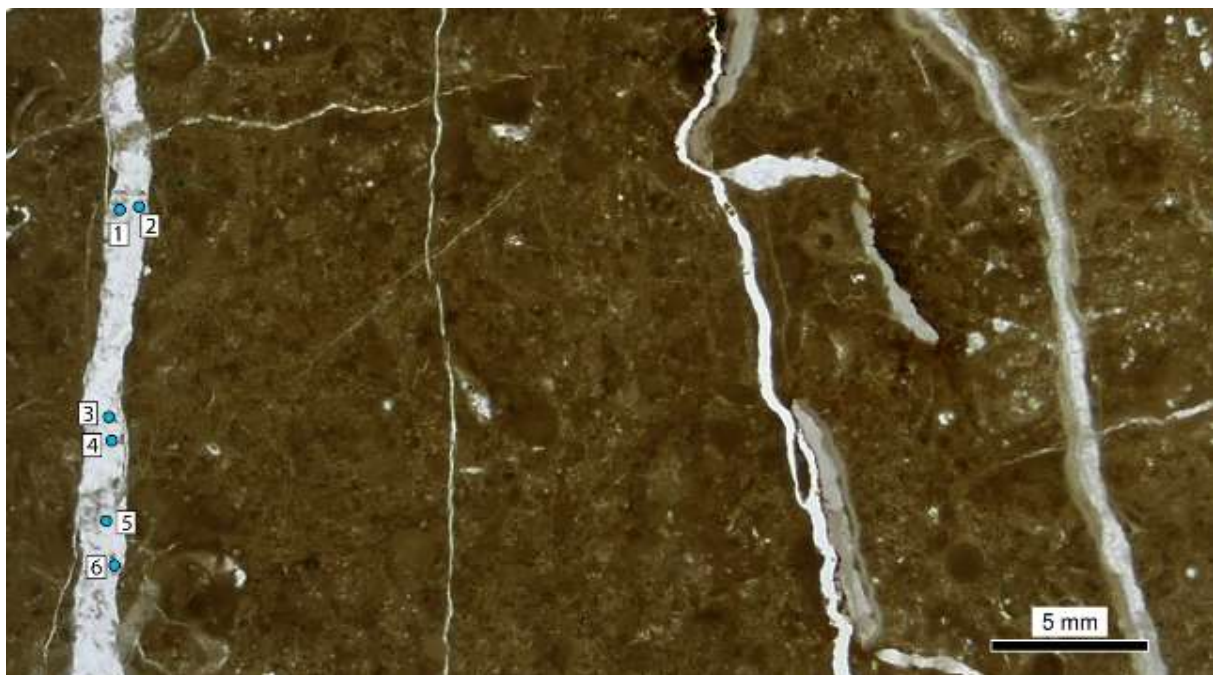

Figure S10 Sample PA7.30B. Structural set: V4. Calcite generations: Cal-1b.

Tables S1-S7

Tables S1-S7 are available as separate .csv files.

Table S1 Geographic location of the 154 samples. The table includes geographic coordinates (WGS84 Decimal Degrees and WGS84 UTM ZONE 32N EPSG:32632) and International Geo Sample Numbers (IGSNs) for each sample.

Table S2 Stable isotope data (Carbon and Oxygen) of various calcite generations and host rocks shown in **Figures 7a-c** and summarized in **Table 1.** Stable carbon and oxygen isotopes are reported in the conventional delta notation with respect to the international standard Vienna Pee Dee Belemnite (V-PDB). Oxygen isotopes are given also with respect to the international standard Standard Mean Ocean Water (SMOW).

Table S3 $^{87}Sr/^{86}Sr$ ratios of various calcite generations and host rocks from Sr isotope analyses performed in situ by laser ablation and in solution from powdered samples by multi-collector-inductively coupled plasma mass spectrometer. For in situ LA-ICP-MS analyses, line numbers correspond to those reported in **Figures S1-S10**. In solution analyses of powdered samples are marked by "sol" after the sample IDs. Errors are given as the double standard error (2SD) that is the internal analytical error of each measurement. Data of calcite cements sampled in deformation structures are ordered according to their petrographic classification (Cal-1/Cal-5). The structural set to which they belong is specified after the sample IDs. These data are plotted in **Figures 8a-b** and summarized in **Table 2**.

Table S4 Summary of clumped isotope analyses. Results are reported in the CDES (Carbon Dioxide Equilibrium Scale). Temperatures were calculated using the Kele *et al*. (2015) calibration, recalculated with the revised IUPAC parameters and the accepted values for the ETH standards, as reported in Bernasconi *et al.* (2018). SD, Standard Deviation; SE, Standard Error; CL, Confidence Level. Data of calcite cements sampled in deformation structures are ordered according to their petrographic classification (Cal-1/Cal-5). The structural set to which they belong is specified in a separate column. $\delta^{18}O$ of the fluid was calculated using the equations reported in Kim and O'Neil (1997), Daëron *et al.* (2019), Kele *et al.* (2015), O'Neil *et al.* (1969). These data are plotted in **Figures 10a-b** and summarized in **Table 3**.

Table S5 Results of clumped isotopes analyses including all the replicates that were measured for each sample. Temperatures were calculated using the Kele et al. (2015) calibration, recalculated with the revised IUPAC parameters and the accepted values for the ETH standards, as reported in Bernasconi et al. (2018). SD, Standard Deviation; SE, Standard Error; CL, Confidence Level. Data of calcite cements sampled in deformation structures are ordered according to their petrographic

classification (Cal-1/Cal-5). For each generation of calcite, mean temperatures and mean δ ^{18}O of the fluids were calculated. These data are summarized in **Table 3**.

Table S6 Results of major and trace element analyses carried out on different generations of calcite and host rocks by laser ablation and in solution from powdered samples. Concentrations are expressed in ppm. Data of calcite cements sampled in deformation structures are ordered according to their petrographic classification (Cal-1/Cal-5). The structural set to which they belong is specified in a separate column. Na, not analysed; bd, below detection limit. REE are normalized to Post Archean Australian Shales (PAAS, Taylor and McLennan, 1985). Ce/Ce* and Eu/Eu* anomalies were calculated according to Tostevin *et al.* (2016).

Table S7 Molar ratios Fe/Ca, Mg/Ca, Sr/Ca, Mn/Ca for the various calcite cements and for the parental fluids. Molar ratios for the fluids were calculated from those of the calcite cements using the formula of McIntire 1963. Kd values for Fe, Mg, Sr and Mn in calcite were calculated through temperatures from Δ47 using the equation of Rimstidt *et al.* (1998).

References

Bernasconi, S. M., Müller, I. A., et al. 2018. Reducing uncertainties in carbonate clumped isotope analysis through consistent carbonate-based standardization. Geochemistry, Geophysics, Geosystems, 19(9), 2895-2914, https://doi.org/10.1029/2017GC007385.

Daëron, M., Drysdale, R. N., Peral, M., Huyghe, D., Blamart, D., Coplen, T. B., Lartaud, F. & Zanchetta, G. 2019. Most Earth-surface calcites precipitate out of isotopic equilibrium. Nature communications, 10(1), 1-7, https://doi.org/10.1038/s41467-019-08336-5.

Kele, S., Breitenbach, S.F.M., et al. 2015. Temperature dependence of oxygen- and clumped isotope fractionation in carbonates: A study of travertines and tufas in the 6-95°C temperature range. Geochimica et Cosmochimica Acta, 168, 172–192, https://doi.org/10.1016/j.gca.2015.06.032.

Kim, S. T., & O'Neil, J. R. 1997. Equilibrium and non equilibrium oxygen isotope effects in synthetic carbonates. Geochimica et cosmochimica acta, 61(16), 3461-3475.

McIntire, W.L. 1963. Trace element partition coefficients-a review of theory and applications to geology. Geochimica et Cosmochimica Acta, 27, 1209–1264, https://doi.org/10.1016/0016-7037(63)90049-8.

O'Neil, J.R., Clayton, R.N. and Mayeda, T.K. 1969. Oxygen isotope fractionation in divalent metal carbonates. The Journal of Chemical Physics, 51, 5547–5558, https://doi.org/10.1063/1.1671982.

Rimstidt, J.D., Balog, A. and Webb, J. 1998. Distribution of trace elements between carbonate minerals and aqueous solutions. Geochimica et Cosmochimica Acta, 62, 1851–1863, https://doi.org/10.1016/S0016-7037(98)00125-2.

Taylor, S.R. and McLennan, S.M. 1985. The Continental Crust: Its Composition and Evolution. Blackwell, Oxford.

Tostevin, R., Shields, G.A., Tarbuck, G.M., He, T., Clarkson, M.O. and Wood, R.A. 2016. Effective use of cerium anomalies as a redox proxy in carbonate-dominated marine settings. Chemical Geology, 438, 146–162, https://doi.org/10.1016/j.chemgeo.2016.06.027.